Tension between $e^+e^- \to \eta\pi^-\pi^+$ and $\tau^- \to \eta\pi^-\pi^0\nu_\tau$ data and nonstandard interactions

Saray Arteaga,[1] Ling-Yun Dai,[2,3] Adolfo Guevara,[4] and Pablo Roig[5]

[1]*The University of Kansas, Department of Physics and Astronomy, 1082 Malott Hall, 1251 Wescoe Hall Drive, Lawrence, Kansas 66045, USA*
[2]*School of Physics and Electronics, Hunan University, Changsha 410082, China*
[3]*Hunan Provincial Key Laboratory of High-Energy Scale Physics and Applications, Hunan University, Changsha 410082, China*
[4]*Institute of Theoretical Physics, Chinese Academy of Sciences, Beijing 100190, China*
[5]*Departamento de Física, Centro de Investigación y de Estudios Avanzados del Instituto Politécnico Nacional, Apdo. Postal 14-740, 07000 Ciudad de México, México*

(Received 9 October 2022; accepted 20 October 2022; published 17 November 2022)

We show the discrepancy between the isospin-rotated $e^+e^- \to \eta\pi^-\pi^+$ cross section—measured by various collaborations—and the Belle $\tau^- \to \eta\pi^-\pi^0\nu_\tau$ spectrum, which cannot be explained by heavy new physics nonstandard interactions. We give for the first time the framework needed to study these beyond the standard model contributions in three-meson tau decays.

DOI: 10.1103/PhysRevD.106.096016

I. INTRODUCTION

In the very accurate isospin symmetry limit, the $e^+e^- \to$ hadrons cross section is related to the spectral function of semileptonic tau decays (see, e.g., Ref. [1]). Beyond tests of this property, based on the conservation of the vector current (CVC), it gave rise to tau-based evaluations of the leading-order hadronic vacuum polarization (HVP, LO) contributions to the muon g-2 [2–9], $a_\mu = (g_\mu - 2)/2$. However, uncertainties associated to isospin-breaking effects relating both observables are currently too large to make this determination competitive with the one using hadronic e^+e^- cross section data [10–17]. Notwithstanding, checking the consistency between $\sigma(e^+e^- \to \text{hadrons})$ and exclusive hadron tau decay data is still motivated by the tension exhibited by lattice QCD evaluations [18–20] of $a_\mu^{HVP,LO}$ and the e^+e^--based data-driven extraction [10]. Depending on which number is compared to the experimental average of the recent FNAL measurement [21] and the final result from the BNL experiment [22], new physics significance varies sizeably, between barely one and slightly more than four standard deviations.

In this work, we study the discrepancy—which goes beyond isospin breaking effects—between both sets of data (e^+e^- and τ) for the exclusive $\eta\pi\pi$ channels, and show that it cannot be explained by heavy new physics.

The isovector component ($I = 1$) of the $e^+e^- \to \eta\pi^+\pi^-$ cross section data can be converted to the decay distribution in $\tau^- \to \eta\pi^-\pi^0\nu_\tau$ decays using the approximate CVC, which becomes exact in the isospin symmetry limit [1,23–26]:

$$\frac{d\Gamma(\tau^- \to \eta\pi^-\pi^0\nu_\tau)}{dQ^2} = f(Q^2)\sigma(e^+e^- \to \eta\pi^+\pi^-)|_{I=1}(Q^2),$$
$$f(Q^2) = \frac{G_F^2|\widetilde{V_{ud}}|^2 S_{\mathrm{EW}}}{(2\pi)^5 M_\tau}\frac{\pi}{4\alpha^2}\left(\frac{M_\tau^2}{Q^2} - 1\right)^2\left(1 + 2\frac{Q^2}{M_\tau^2}\right)Q^6, \tag{1}$$

with $Q^2 = m_{\eta\pi\pi}^2$ the invariant mass squared of the $\eta\pi\pi$ system and $S_{\mathrm{EW}} = 1.0201(3)$ [27] the short-distance electroweak radiative correction. We note that $\widetilde{V_{ud}}$ differs from V_{ud} by possible nonstandard effects (see Sec. II).

Using Eq. (1), Belle [28] data on $\tau^- \to \eta\pi^-\pi^0\nu_\tau$ decays are seen to be incompatible with $e^+e^- \to \eta\pi^-\pi^+$ measurements published by DM2 [29], ND [30], CMD2 [31], *BABAR* [32], SND [33–35], and CMD3 [36]. We use the best fits obtained in Refs. [37,38] to the $e^+e^- \to (\eta/\pi^0)\pi^+\pi^-$ data for the Standard Model prediction. Since possible heavy new physics effects are negligible compared to the photon exchange driving these processes, a possible discrepancy between the isospin-rotated $e^+e^- \to \eta\pi^+\pi^-$ cross section and the $\tau^- \to \eta\pi^-\pi^0\nu_\tau$ decay rate [1,23–25] (besides small isospin breaking effects) could in principle

Published by the American Physical Society under the terms of the Creative Commons Attribution 4.0 International license. Further distribution of this work must maintain attribution to the author(s) and the published article's title, journal citation, and DOI. Funded by SCOAP^3.

be due to nonstandard interactions (NSI) modifying the latter. Thanks to the limits set on possible NSI in semileptonic tau decays [39–47] we will show that this seeming CVC violation is incompatible with other hadron tau decays data. Belle-II will improve the measurement of this tau decay channel [48], as understanding semileptonic tau decays with eta mesons is required to search for second-class currents and heavy new physics through the discovery of the $\tau^- \to \pi^- \eta^{(\prime)} \nu_\tau$ decays [39,49,50]. The rest of the paper is structured as follows: in Sec. II we briefly recall the formalism encoding nonstandard interactions in semileptonic tau decays. In Sec. III we derive the $\tau^- \to \eta\pi^-\pi^0\nu_\tau$ decays amplitude, in the Standard Model and including the NSI (involving new hadron contributions, which we account for). In Sec. IV we study the possible effects of NSI on the observables of interest, and show that the discrepancy between e^+e^- and τ data cannot be explained by heavy new physics, according to the NSI bounds. We conclude in Sec. V. The Appendix summarizes the setting in which structure-dependent contributions were evaluated.

II. EFFECTIVE FIELD THEORY ANALYSIS OF NSI IN SEMILEPTONIC TAU DECAYS

We consider the most general effective field theory description of $\tau^- \to \bar{u} d \nu_\tau$ decays,[1] assuming massless purely left-handed neutrinos [39–47] (see, e.g., Refs. [51–61] for other semileptonic processes involving light quarks within this framework), which only rests on the $SU(3)_C \times U(1)$ local gauge symmetry below the electroweak scale. For later convenience we introduce $\epsilon_V \coloneqq \epsilon_L + \epsilon_R$ and $\epsilon_A \coloneqq -\epsilon_L + \epsilon_R$, so that the relevant Lagragian at dimension six is

$$\mathcal{L} = -\frac{G_F \widetilde{V_{ud}}}{\sqrt{2}} \{ \bar{\tau}\gamma^\mu (1-\gamma_5)\nu_\tau \cdot [\bar{u}\gamma_\mu(1-\gamma_5)d + \bar{u}\gamma_\mu(\epsilon_V^\tau + \epsilon_A^\tau \gamma_5)d] + \bar{\tau}(1-\gamma_5)\nu_\tau \cdot \bar{u}(\epsilon_S^\tau - \epsilon_P^\tau \gamma_5)d + 2\epsilon_T^\tau \bar{\tau}\sigma^{\mu\nu}(1-\gamma_5)\nu_\tau \cdot \bar{u}\sigma_{\mu\nu} d \} + \text{H.c.}, \tag{2}$$

where $G_F V_{ud} = G_F \widetilde{V_{ud}}(1+\epsilon_V^e)$ [61]. We neglect higher-dimensional operators, suppressed by powers of M_τ/Λ, since current limits on the ϵ_i coefficients [39–47] correspond to $\Lambda \sim \mathcal{O}(\text{TeV})$ (under the weak-coupling hypothesis). As we only compute CP-conserving observables,[2] the ϵ_i coefficients are taken real. They are translated straightforwardly [51,58] into the SMEFT [66,67] couplings. For vanishing ϵ_i, the SM is recovered. We will work in the $\overline{\text{MS}}$ scheme at a scale of $\mu = 2$ GeV.

III. $\tau^- \to \eta\pi^-\pi^0\nu_\tau$ AMPLITUDE

We will assign momenta as[3] $\tau^-(P) \to \nu_\tau(p_1)\eta(p_2) \times \pi^-(p_3)\pi^0(p_4)$ and use Kumar kinematics [68],[4] so that the outermost integration variable, $(P-p_1)^2 = (p_2+p_3+p_4)^2$, gives us $Q^2 = m^2_{\eta\pi\pi}$, whose distribution was measured by Belle [28].

A. Hadronization: Standard Model and beyond

In the Standard Model, the $\tau^- \to \eta\pi^-\pi^0\nu_\tau$ decay amplitude is

$$\mathcal{M} = -\frac{G_F}{\sqrt{2}} V_{ud} \sqrt{S_{\text{EW}}}\, \bar{u}_{\nu_\tau}\gamma^\mu(1-\gamma_5)u_\tau \mathcal{H}_\mu, \tag{3}$$

where $\mathcal{H}_\mu$ encodes the hadronization into the three final-state mesons ($h_1 = \eta, h_2 = \pi^-, h_3 = \pi^0$ in our case and with our conventions). Lorentz invariance determines the most general decomposition of $\mathcal{H}^\mu$ to be

$$\begin{aligned}\mathcal{H}^\mu &= \langle h_1(p_2)h_2(p_3)h_3(p_4)|(V-A)^\mu|0\rangle \\ &= F_1^A(Q^2,s_2,t_3')V_1^\mu + F_2^A(Q^2,s_2,t_3')V_2^\mu \\ &\quad + iF_3^V(Q^2,s_2,t_3')V_3^\mu + F_4^A(Q^2,s_2,t_3')Q^\mu,\end{aligned} \tag{4}$$

where the chosen set of independent Lorentz structures is

$$\begin{aligned} V_1^\mu &= \left(g^{\mu\nu} - \frac{Q^\mu Q^\nu}{Q^2}\right)(p_2 - p_4)_\nu, \\ V_2^\mu &= \left(g^{\mu\nu} - \frac{Q^\mu Q^\nu}{Q^2}\right)(p_3 - p_4)_\nu, \\ V_3^\mu &= \varepsilon_{\mu\alpha\beta\gamma} p_2^\alpha p_3^\beta p_4^\gamma, \qquad Q^\mu = (p_2+p_3+p_4)^\mu, \\ s_2 &= (Q-p_2)^2, \qquad t_3' = (p_2+p_4)^2, \end{aligned} \tag{5}$$

and the relevant form factors ($F_i, i = 1, \ldots, 4$) are driven by either vector or axial-vector currents (as indicated by their

[1] Hadronic interactions will be considered in the next section.

[2] See, e.g., Refs. [42,62–65] for studies of CP violation in $\tau \to K_S\pi\nu_\tau$ decays within this low-energy effective field theory.

[3] Unlike Ref. [68], we do not use Q as the momentum of the decaying particle, since this corresponds to the invariant mass of the $\eta\pi\pi$ system in our notation.

[4] In Ref. [69] it was shown that the kinematics adopted in, e.g., Ref. [25] is not appropriate when tensor interactions are considered, as the factorization of the lepton and hadron parts (with the latter only depending on three independent invariants, which can be written in terms of the meson momenta) no longer holds.

superscript, V/A) and carry quantum numbers of pseudoscalar (F_4), vector (F_3), or axial-vector ($F_{1,2}$) degrees of freedom. Very approximate G-parity conservation by the strong interactions[5] produces vanishing axial-vector form factors in this channel, in such a way that—to an excellent accuracy—the dynamics of the considered decays are driven solely by the vector form factor, F_3, which will be taken from the best fits of Refs. [37,38].

As explained, $F^A_{1,2,4}$ vanish in the limit of G-parity conservation. We will however compute the isospin-breaking contributions to these form factors given by scalar resonance exchanges. Our motivation to include these subleading effects only for the scalar mesons contributions is twofolded: on the one hand isospin-violating $f_0 - a_0$ mixing is enhanced with respect to other isospin breaking effects by the approximate degeneracy of these states and their comparable value to the kaon-antikaon thresholds [70]. On the other hand, Belle-II shall measure the dimeson mass spectra[6] in $\tau^- \to \eta\pi^-\pi^0\nu_\tau$ decays and a theoretically motivated parametrization of scalar meson exchanges in these processes will benefit their analysis. In this way, we will construct the hadronic input needed for NSI contributions to the considered decays.

There are three possible contributions with intermediate scalar resonances (all of them in the axial-vector current), one per channel. Schematically, they are

1. $A^\mu \to a_0^-\eta$, with $a_0^- \to \pi^-\pi^0$ via $\eta^{(\prime)} - \pi^0$ mixing, in the s_1 channel ($T^\alpha_{s_1}$ below).
2. $A^\mu \to a_0^0\pi^-$, with $a_0^0 \to \pi^0\eta^{(\prime)}$ via $f_0 - a_0$ mixing, in the s_2 channel ($T^\alpha_{s_2}$ below).
3. $A^\mu \to a_0^-\pi^0$, with $a_0^- \to \pi^-\eta^{(\prime)}$ via $\eta^{(\prime)} - \pi^0$ mixing, in the s_3 channel ($T^\alpha_{s_3}$ below).

The corresponding scalar resonance exchange contributions, computed within resonance chiral theory [73] ($R\chi$T, see the Appendix), are

$$
\begin{aligned}
T^\alpha_{s_1} &= p_2^\alpha \frac{4\sqrt{2}C_{q^{(\prime)}}}{F^3}\frac{C_q\epsilon_{\pi\eta} + C_{q'}\epsilon_{\pi\eta'}}{M^2_{a_0} - s_1 - iM_{a_0}\Gamma_{a_0}(s_1)} c_d\left[c_d\left(\frac{s_1}{2} - m_\pi^2\right) + c_m m_\pi^2\right],\\
T^\alpha_{s_2} &= p_3^\alpha \frac{4\sqrt{2}C_{q^{(\prime)}}}{\sqrt{3}F^3}\frac{\epsilon_{a_0f_0}(s_2)}{M^2_{a_0} - s_2 - iM_{a_0}\Gamma_{a_0}(s_2)} c_d\left[c_d\left(\frac{s_2 - m_\pi^2 - m_\eta^2}{2}\right) + c_m m_\pi^2\right],\\
T^\alpha_{s_3} &= p_4^\alpha \frac{4\sqrt{2}C_{q^{(\prime)}}}{F^3}\frac{C_q\epsilon_{\pi\eta} + C_{q'}\epsilon_{\pi\eta'}}{M^2_{a_0} - s_3 - iM_{a_0}\Gamma_{a_0}(s_3)} c_d\left[c_d\left(\frac{s_3 - m_\pi^2 - m_\eta^2}{2}\right) + c_m m_\pi^2\right],
\end{aligned}
\tag{6}
$$

where [74] $\epsilon_{a_0f_0}(s_2) = \epsilon_{a_0f_0}(\sigma_{K^0}(s_2) - \sigma_{K^+}(s_2))/2$, with $\epsilon_{a_0f_0} \sim \mathcal{O}(1)$.[7] Short-distance QCD constraints set $4c_dc_m = F^2$ [77,78] (with $F \sim 92$ MeV) and $c_m \sim 3c_d$ is preferred phenomenologically (see [79] and references therein). $C_{q^{(\prime)}}$ are given in terms of the $\eta - \eta'$ mixing parameters [80]

$$
\begin{aligned}
C_q &\equiv \frac{1}{\sqrt{3}\cos(\theta_8 - \theta_0)}\left(\frac{\cos\theta_0}{f_8} - \frac{\sqrt{2}\sin\theta_8}{f_0}\right),\\
C_{q'} &\equiv \frac{1}{\sqrt{3}\cos(\theta_8 - \theta_0)}\left(\frac{\sqrt{2}\cos\theta_8}{f_0} + \frac{\sin\theta_0}{f_8}\right),
\end{aligned}
\tag{7}
$$

and $\varepsilon_{\pi\eta} = (9.8 \pm 0.3) \times 10^{-3}$ and $\varepsilon_{\pi\eta'} = (2.5 \pm 1.5) \times 10^{-4}$ [50]. We will take the numerical values for $C_{q^{(\prime)}}$ from Ref. [81] (see also Ref. [82]): $C_q = 0.69 \pm 0.03$ and $C_{q'} = 0.60 \pm 0.03$, obtained in the chiral limit.

The $\Gamma_{a_0}(s_i)$ energy-dependent width is given by [50]

$$
\Gamma_{a_0}(s_i) = \Gamma_{a_0}(M^2_{a_0})\left(\frac{s_i}{M^2_{a_0}}\right)^{3/2}\frac{h(s_i)}{h(M^2_{a_0})},
\tag{8}
$$

with ($\sigma_{PQ}(s_i) = \lambda^{1/2}(s_i, m_P^2, m_Q^2)/s \times \Theta(s_i - (m_P + m_Q)^2)$ is a kinematical factor and $\lambda(a,b,c) = (a-b-c)^2 - 4bc$)

$$
\begin{aligned}
h(s_i) &= \sigma_{K^-K^0}(s_i) + 2\cos^2\phi_{\eta\eta'}\left(1 + \frac{\Delta_{\pi^-\eta}}{s_i}\right)^2\sigma_{\pi^-\eta}(s_i)\\
&\quad + 2\sin^2\phi_{\eta\eta'}\left(1 + \frac{\Delta_{\pi^-\eta'}}{s_i}\right)^2\sigma_{\pi^-\eta'}(s_i),
\end{aligned}
\tag{9}
$$

[5] G parity is built from C parity and isospin symmetry. For consistency, ignoring the effect of the $F_{1,2,4}$ form factors requires to describe F_3 in the isospin symmetry limit.

[6] Unexpectedly, Belle [28] found a disagreement between their measured $\pi^-\pi^0$ spectra and the Monte Carlo event generator [71,72], validated with precise previous data on the weak pion vector form factor.

[7] $T^\alpha_{s_2}$ has been obtained assuming, for simplicity, that $f_0(980)$ is a pure octet state. If it comes from the mixing of the octet and singlet f states, then the corresponding mixing coefficient can be absorbed in the constant $\epsilon_{a_0f_0}$, which we will fix to unity for definiteness. This and other ambiguities present in the description of the scalar mesons (like possible tetraquark components [75] and more complicated mixing pattern [76]) prevent us from attempting to derive the real part of the meson-meson loops, which should be present in the a_0 propagators in Eq. (6) to fulfill analyticity.

$\Delta_{PQ} = m_P^2 - m_Q^2$ and $\phi_{\eta\eta'} = (41.4 \pm 0.5)^\circ$ [83]. Mass and on-shell width of the a_0 resonance will be taken from the PDG [75]. Scalar contributions in Eq. (6) can be written in terms of the $F^A_{1,2,4}$ form factors using

$$\begin{aligned}
p_2^\mu &= \frac{Q^\mu}{2Q^2}(Q^2 - s_1 + m_\eta^2) + \frac{2V_1^\mu}{3} - \frac{V_2^\mu}{3},\\
p_3^\mu &= \frac{Q^\mu}{2Q^2}(Q^2 - s_2 + m_\pi^2) - \frac{V_1^\mu}{3} + \frac{2V_2^\mu}{3},\\
p_4^\mu &= \frac{Q^\mu}{2Q^2}(s_1 + s_2 - m_\eta^2 - m_\pi^2) - \frac{V_1^\mu}{3} - \frac{V_2^\mu}{3}.
\end{aligned} \tag{10}$$

For consistency—as scalar resonance contributions are included—axial-vector current contributions induced from $\tau^- \to \pi^-\pi^0\pi^0$ decays coming from $\pi^0 - \eta$ mixing need to be accounted for as well. This is done following Refs. [84–86] (including also the $KK\pi$ cuts [87] into the energy-dependent Γ_{a_1}). The overall factor $\epsilon_{\pi\eta}^2$ suppresses strongly this contribution, which does not introduce any additional free parameter.

Beyond the Standard Model, the vector and axial-vector matrix elements (corresponding to the $\bar{d}\gamma^\mu u$ and $\bar{d}\gamma^\mu\gamma_5 u$ quark currents) can be written in terms of the $\{F_i\}_{i=1,\ldots,4}$ form factors (we omit their dependence on Q^2, s_1, s_2 below)

$$\begin{aligned}
H_V^\mu &= iF_3^{V,\mathrm{NSI}} V_3^\mu,\\
-H_A^\mu &= F_1^{A,\mathrm{NSI}} V_1^\mu + F_2^{A,\mathrm{NSI}} V_2^\mu + F_4^{A,\mathrm{NSI}} Q^\mu,
\end{aligned} \tag{11}$$

which are defined by the currents

$$H^\mu_{(V/A)} = \epsilon_{(V/A)} \langle \eta\pi^-\pi^0 | \bar{d}\gamma^\mu(1,\gamma_5)u|0\rangle. \tag{12}$$

We can relate the previous terms with the hadronization in Eq. (3) with the relation

$$\mathcal{H}^\mu = H^\mu_{\mathrm{NSI}} + H^\mu_L, \tag{13}$$

where H_L contains all SM interactions and $H^\mu_{V/A} \in H_{\mathrm{NSI}}$. The (pseudo)scalar matrix elements can be related to the former using Dirac equation. This shows the vanishing of the hadron matrix element of the scalar current, while the pseudoscalar one (for the $\bar{d}\gamma_5 u$ quark current) can be related to H_A^μ, which is defined as

$$H_P = \epsilon_P \langle \eta\pi^-\pi^0 | \bar{d}\gamma_5 u|0\rangle, \tag{14}$$

yielding

$$H_P = \frac{F_4^A Q^2}{m_u + m_d}. \tag{15}$$

We will finally address the hadronization of the tensor current ($\langle \eta\pi^-\pi^0 | \bar{d}\sigma^{\mu\nu}u|0\rangle$) for which we will employ chiral perturbation theory [88] with tensor sources [89]. The leading contribution in the chiral counting is given in terms of a single coupling constant, Λ_2, which can be determined from the lattice [90] to be $\Lambda_2 = (11.1 \pm 0.4)$ MeV [43]. In terms of it, the hadron matrix element for the tensor current is

$$H_T^{\mu\nu} = i\frac{\Lambda_2 C_q}{\sqrt{2}F^3}\epsilon^{\mu\nu\alpha\beta}(p_{3\alpha}p_{2\beta} - p_{2\alpha}p_{3\beta}). \tag{16}$$

B. Decay amplitude

The $\tau^- \to \eta\pi^-\pi^0\nu_\tau$ decay amplitude can be written[8]

$$\begin{aligned}
\mathcal{M} &= \mathcal{M}_{\mathrm{SM}} + \mathcal{M}_V + \mathcal{M}_A + \mathcal{M}_P + \mathcal{M}_T,\\
&= -\frac{G_F \widetilde{V_{ud}}\sqrt{S_{\mathrm{EW}}}}{\sqrt{2}}[L_\mu(H^\mu + \epsilon_V H_V^\mu + \epsilon_A H_A^\mu)\\
&\quad - \epsilon_P L H_P + 2\epsilon_T L_{\mu\nu}H^{\mu\nu}],
\end{aligned} \tag{17}$$

where the following lepton currents were introduced

$$\begin{aligned}
L &= \bar{u}(p_1)(1+\gamma_5)u(P), \qquad L_\mu = \bar{u}(p_1)\gamma_\mu(1-\gamma_5)u(P),\\
L_{\mu\nu} &= \bar{u}(p_1)\sigma_{\mu\nu}(1+\gamma_5)u(P).
\end{aligned} \tag{18}$$

Using the Dirac equation, $L_\mu Q^\mu = M_\tau L$ is obtained. This, together with Eq. (15), allows the convenient rewriting $\epsilon_A L_\mu H_A^\mu - \epsilon_P L H_P = \epsilon_A L_\mu H'^\mu_A$, where

$$H'^\mu_A = H_A^\mu - \frac{\epsilon_P}{\epsilon_A}\frac{F_4^A Q^2 Q^\mu}{M_\tau(m_u + m_d)}, \tag{19}$$

which in turn allows us to recast Eq. (17) as

$$\begin{aligned}
\mathcal{M} &= \mathcal{M}_{\mathrm{SM}} + \mathcal{M}_V + \mathcal{M}_{A'} + \mathcal{M}_T,\\
&= -\frac{G_F \widetilde{V_{ud}}\sqrt{S_{\mathrm{EW}}}}{\sqrt{2}}[L_\mu(H^\mu + \epsilon_V H_V^\mu + \epsilon_A H'^\mu_A)\\
&\quad + 2\epsilon_T L_{\mu\nu}H^{\mu\nu}],
\end{aligned} \tag{20}$$

which we have used to compute the observables presented in the following section. We provide Supplemental Material [91] with the analytic results for the different contributions to $|\mathcal{M}|^2$, for which we used FeynCalc [92–94].

IV. CVC PREDICTION OF THE $\tau^- \to \eta\pi^-\pi^0\nu_\tau$ DECAY RATE AND NSI

For our isospin-rotated prediction of the $\tau^- \to \eta\pi^-\pi^0\nu_\tau$ decays in absence of new physics we will use the CVC

[8]Although the effect of the short-distance radiative electroweak corrections encoded in S_{EW} affects only the SM contribution, we approximate it as a global factor in the equation below. Its accuracy is sufficient for our precision and renders simpler expressions.

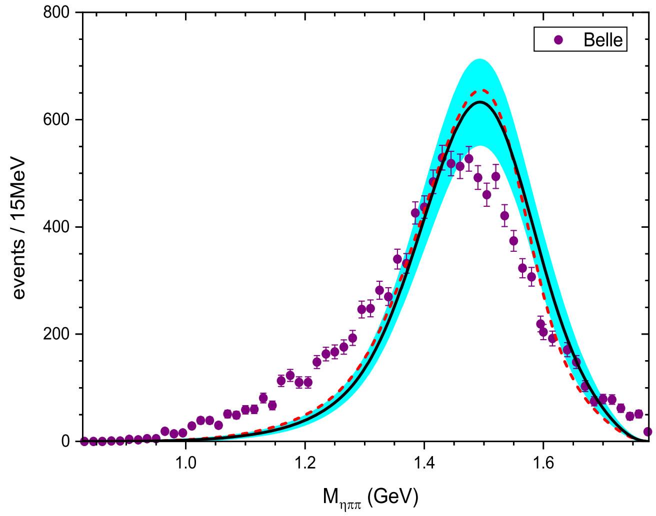

FIG. 1. The prediction of $\tau^- \to \eta\pi^-\pi^0\nu_\tau$ from $e^+e^- \to \eta\pi^+\pi^-$ amplitudes. The black solid line is calculated from Fit II of Ref. [38] and the red dashed line is from Fit 4 of Ref. [37]. The cyan band describes the uncertainty obtained by a combined statistics of the error band of Fit II in Ref. [38] and the difference between the red and black lines. Belle data are represented by purple dots.

relation [see Eq. (1)], with $e^+e^- \to \eta\pi^+\pi^-$ given by the best fit solutions of Refs. [37,38] (see also Ref. [95]). Specifically, Fit 4 in Ref. [37] and Fit II in Ref. [38], respectively. The amplitudes were calculated using RχT [73] and confronted with the latest high statistics experimental measurements of $e^+e^- \to \eta\pi^+\pi^-$ cross sections up to 2.3 GeV, including those of *BABAR* [32], SND [33,35], and CMD3 [36]. By isospin rotation, the prediction of the invariant mass spectrum of $\tau^- \to \eta\pi^-\pi^0\nu_\tau$ decays is given in Fig. 1. It can be seen that the prediction from $e^+e^- \to \eta\pi^+\pi^-$ is quite different from that of the Belle data [28], especially in the region of 0.9–1.4 GeV. The $\tau \to \eta\pi^-\pi^0\nu_\tau$ branching ratio is $(1.71 \pm 0.13) \times 10^{-3}$, using the Fit II in Ref. [38], and $(1.55 \pm 0.18) \times 10^{-3}$ from Fit 4 of Ref. [37]. The PDG quotes $(1.39 \pm 0.07) \times 10^{-3}$ instead, from which our previous numbers are 2.2 and 0.8σ away, respectively. Meanwhile, $e^+e^- \to \eta\pi^+\pi^-$ data are considered much more accurate and trustworthy. Hence, it would be rather important for Belle-II to improve the measurement of this decay channel in the future.

The effects of NSI are constrained thanks to the most recent determination (in agreement with previous ones) of these couplings [47], yielding

$$\begin{pmatrix} \epsilon_L^\tau - \epsilon_L^e + \epsilon_R^\tau - \epsilon_R^e \\ \epsilon_R^\tau \\ \epsilon_P^\tau \\ \epsilon_T^\tau \end{pmatrix} = \begin{pmatrix} 2.4 \pm 2.6 \\ 0.7 \pm 1.4 \\ 0.4 \pm 1.0 \\ -3.3 \pm 6.0 \end{pmatrix} \times 10^{-2}, \tag{21}$$

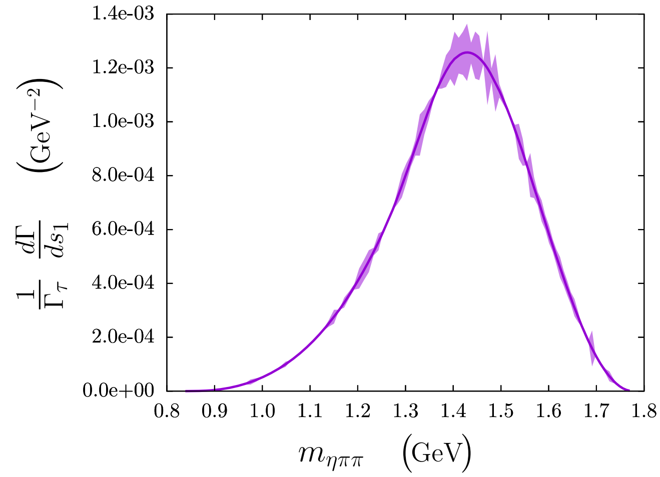

FIG. 2. Invariant mass spectrum of the $\tau^- \to \eta\pi^-\pi^0\nu_\tau$ transition. The purple stripe is the error band obtained from the Gaussian variation of parameters at each bin, the solid purple line represents the mean of the distribution.

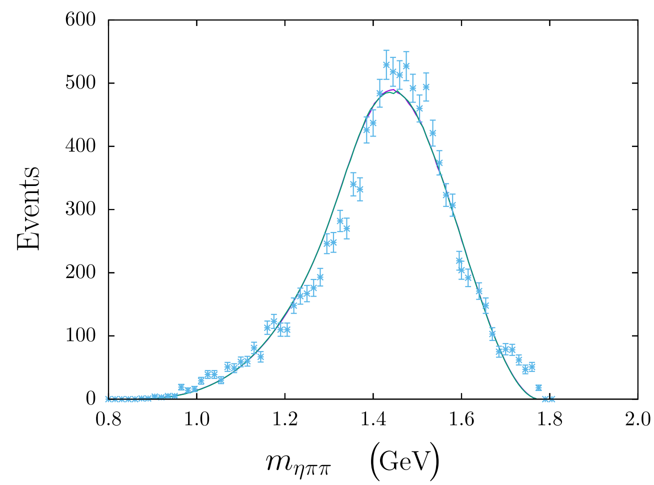

FIG. 3. Comparison between the spectra obtained using the complete amplitude (purple line) with the NSI turned off (green line) and the Belle data (pale blue dots). The difference between both lines can be slightly appreciated only near the peak.

with the correlation matrix

$$C_\epsilon = \begin{pmatrix} 1 & 0.87 & -0.18 & -0.98 \\ & 1 & -0.59 & -0.86 \\ & & 1 & 0.18 \\ & & & 1 \end{pmatrix}. \tag{22}$$

In our numerical analysis we used 2500 points[9] generated randomly following a Gaussian distribution using

[9]This amount of points was chosen to obtain a kurtosis near to 3, getting $K = 3.17$, which guarantees their distribution is Gaussian.

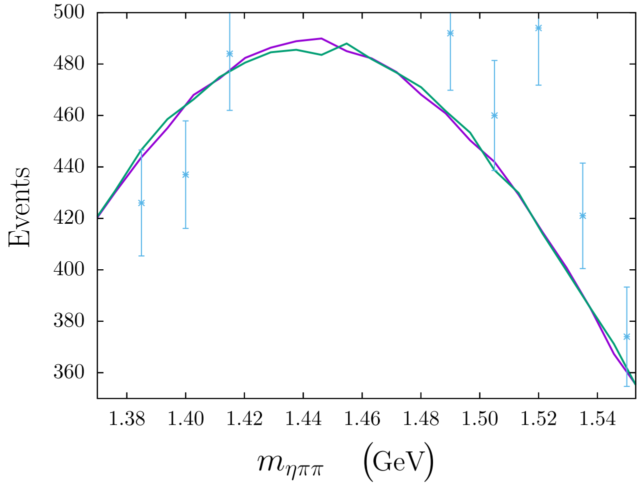

FIG. 4. Enlargement of Fig. 3 in the small region where the data differ.

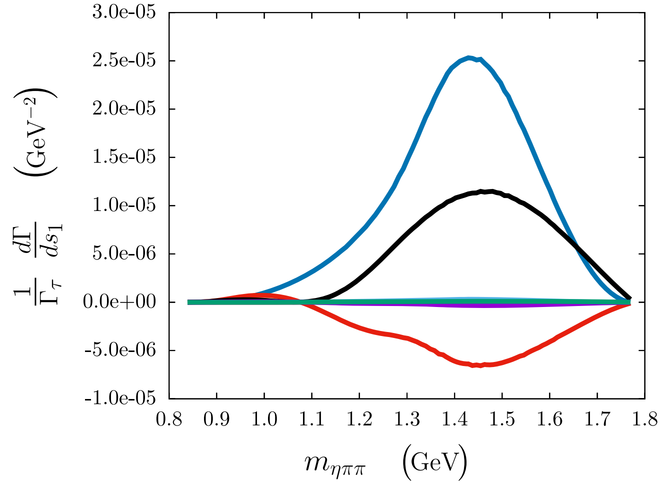

FIG. 6. Same contributions from Fig. 5, without the SM contribution. The color code is the same as in the previous figure.

the parameters and errors in Eq. (21) and the correlation matrix of Eq. (22). The vector form factor in Ref. [25] was used in the following.

We also computed the invariant mass $m_{\eta\pi\pi}$ spectrum for which we again used a Gaussian variation of the parameters, generating 2500 points at each bin of the spectrum, shown in Fig. 2.

When comparing the result of the total differential decay width to that obtained only from the SM contribution to the amplitude and the Belle spectrum, shown in Fig. 3, we confirm that the possible NSI contribution is undetectable with current data. In Fig. 4 we show a close up of the region where both curves of Fig. 3 differ a bit more.

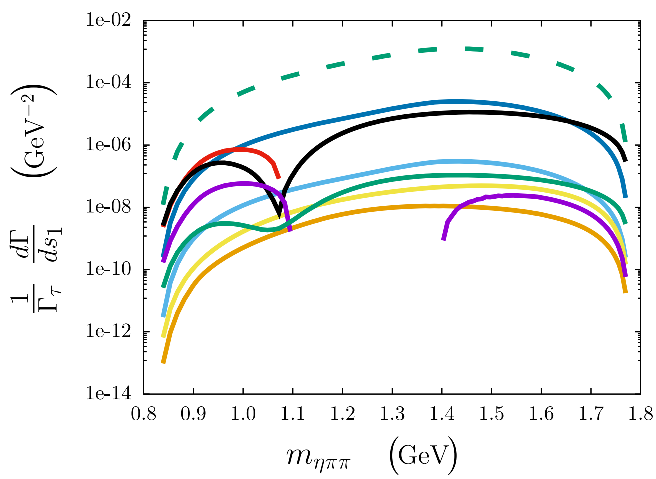

FIG. 5. Different contributions to the differential decay width, shown in a logarithmic scale. Because of this, some of them cannot be shown in this figure, since interference terms are negative in certain regions of the invariant mass range. The color code follows: pure SM (dark green), SM-V (dark blue), SM-A (red), SM-T (black), A-V (lilac), V-T (green), A-T (purple), $|\mathrm{V}|^2$ (pale blue), $|\mathrm{A}|^2$ (yellow), $|\mathrm{T}|^2$ (orange).

We also obtained the contributions to the decay width from the different terms in the squared amplitude, this is, pure V, A, P, T, SM terms or only one of the interference terms among them, in turn. This is shown in Fig. 5 in a logarithmic scale. In Fig. 6 we show all such contributions, except for the pure SM one, in a normal scale. For most of the phase space the interference of the SM with the vector nonSM interaction dominates. At low invariant masses there is a small window where the SM-tensor and SM-axial interferences overcome it slightly. It is also seen that the SM-tensor interference dominates near the end point. It must be noted, however, that the tensor effects at high invariant masses may be smaller than depicted, as we are using for this form factor only the leading order contribution in the chiral expansion. Going beyond this approximation should—in particular—reduce the effects shown for the SM-tensor interference at high $m_{\eta\pi\pi}$. These results can be used to study possible new physics effects in the $\tau^- \to \eta\pi^-\pi^0\nu_\tau$ decays with future improved data.

V. CONCLUSIONS

We have studied whether the discrepancy between isospin-rotated $\sigma(e^+e^- \to \eta\pi^+\pi^-)$ and $d\Gamma(\tau^- \to \eta\pi^+\pi^0\nu_\tau)/dm_{\eta\pi\pi}$ data can be explained by heavy new physics beyond the SM. Within an effective field theory approach for the NSI (assuming left-handed neutrinos), and using the bounds obtained previously on the corresponding new physics couplings, we have shown that it is impossible to explain this tension between e^+e^- and τ data by heavy new physics. Future measurement of the τ decay channel at Belle-II will shed light on the origin of this controversy. As a byproduct of our analysis, we have developed the formalism needed to study NSI in three-meson tau decays (see the Supplemental Material [91]), which can be useful for other decay channels where hadronization is more complicated.

ACKNOWLEDGMENTS

S. A. acknowledges Conacyt for her Ms. Sc. scholarship at Cinvestav. L.-Y. D. is supported by Joint Large Scale Scientific Facility Funds of the National Natural Science Foundation of China (NSFC) and Chinese Academy of Sciences (CAS) under Contract No. U1932110, NSFC Grant No. 12061141006, and Fundamental Research Funds for the Central Universities. P. R. is indebted to Kenji Inami for providing him with Belle data and for clarifying explanations on this analysis, and thanks Michel Hernández Villanueva and Iván Heredia de la Cruz's work on this topic. Useful discussions on this subject with Gabriel López Castro and Antonio Rodríguez Sánchez are also acknowledged. P. R. was partly funded by Conacyt's project within "Paradigmas y Controversias de la Ciencia 2022," Grant No. 319395, and by Cátedra Marcos Moshinsky (Fundación Marcos Moshinsky) 2020, whose support is also acknowledged by A. G.

APPENDIX: BRIEF OVERVIEW OF RESONANCE CHIRAL THEORY

In this appendix we recapitulate briefly the framework in which the model-dependent contributions have been evaluated [25,37,38], RχT [73]. See, for instance Ref. [96] for further details.

Resonances are added as explicit degrees of freedom to the χPT Lagrangian, which is enlarged by terms including them,[10] where the χPT chiral tensors also appear. The symmetries determining the Lagrangian operators are the chiral one for the lightest pseudoscalar mesons (which are pseudo-Goldstone bosons) and unitary symmetry for the resonances, $SU(3)_L \otimes SU(3)_R \to SU(3)_V$ and $U(3)_V$, respectively, for the three lightest quark flavors. The expansion parameter of RχT is the inverse of the number of colors [97], where the leading order corresponds to tree level diagrams with an infinite tower of mesons per quantum number [97,98] (the most important subleading correction comes from finite resonance widths).

Symmetries do not restrict the coupling values, so these should in principle be determined phenomenologically. However, assuming that the theory with resonances can interpolate between the chiral and parton regimes, Green functions in RχT need to comply with the known (from the corresponding operator product expansion) QCD short-distance behavior. This determines or relates some of the couplings, increasing the predictivity of RχT. At the same time, this requirement tightly constrains contributions from operators with high-order chiral tensors. Complementarily, the number of resonance fields is limited by the process at hand (via the number of initial and final state mesons, to which exchanged resonances couple). Altogether, this restricts, in practice, the number of operators of the RχT Lagrangians in the large-N_C limit. The minimal interactions with (pseudo) scalar and (axial) vector resonances are given by [73]

$$\begin{aligned}
\mathcal{L}_V &= \frac{F_V}{2\sqrt{2}}\langle V_{\mu\nu} f_+^{\mu\nu}\rangle + i\frac{G_V}{\sqrt{2}}\langle V_{\mu\nu} u^\mu u^\nu\rangle, \\
\mathcal{L}_A &= \frac{F_A}{2\sqrt{2}}\langle A_{\mu\nu} f_-^{\mu\nu}\rangle, \\
\mathcal{L}_S &= c_d\langle S u^\mu u_\mu\rangle + c_m\langle S\chi_+\rangle, \\
\mathcal{L}_P &= i d_m\langle P\chi_-\rangle,
\end{aligned} \tag{A1}$$

see Ref. [73] for further details.

Recent applications of RχT include Refs. [8,38,45,46,81,99–103], mostly focused on tau decays and hadronic contributions to the muon g-2.

[10] We note that χPT operators coefficients are different in RχT according to the contributions, to the χPT low-energy constants, of integrating resonances out.

[1] S. I. Eidelman and V. N. Ivanchenko, Phys. Lett. B **257**, 437 (1991).
[2] R. Alemany, M. Davier, and A. Höcker, Eur. Phys. J. C **2**, 123 (1998).
[3] V. Cirigliano, G. Ecker, and H. Neufeld, Phys. Lett. B **513**, 361 (2001).
[4] V. Cirigliano, G. Ecker, and H. Neufeld, J. High Energy Phys. 08 (2002) 002.
[5] M. Davier, A. Hoecker, G. López Castro, B. Malaescu, X. H. Mo, G. Toledo Sánchez, P. Wang, C. Z. Yuan, and Z. Zhang, Eur. Phys. J. C **66**, 127 (2010).
[6] M. Davier, A. Hoecker, B. Malaescu, and Z. Zhang, Eur. Phys. J. C **71**, 1515 (2011); **72**, 1874(E) (2012).
[7] M. Davier, A. Höcker, B. Malaescu, C. Z. Yuan, and Z. Zhang, Eur. Phys. J. C **74**, 2803 (2014).
[8] J. A. Miranda and P. Roig, Phys. Rev. D **102**, 114017 (2020).
[9] M. Benayoun, L. DelBuono, and F. Jegerlehner, Eur. Phys. J. C **82**, 184 (2022).
[10] T. Aoyama, N. Asmussen, M. Benayoun, J. Bijnens, T. Blum, M. Bruno, I. Caprini, C. M. Carloni Calame, M. Cè, G. Colangelo *et al.*, Phys. Rep. **887**, 1 (2020).
[11] M. Davier, A. Hoecker, B. Malaescu, and Z. Zhang, Eur. Phys. J. C **77**, 827 (2017).
[12] A. Keshavarzi, D. Nomura, and T. Teubner, Phys. Rev. D **97**, 114025 (2018).

[13] G. Colangelo, M. Hoferichter, and P. Stoffer, J. High Energy Phys. 02 (2019) 006.
[14] M. Hoferichter, B. L. Hoid, and B. Kubis, J. High Energy Phys. 08 (2019) 137.
[15] M. Davier, A. Hoecker, B. Malaescu, and Z. Zhang, Eur. Phys. J. C **80**, 241 (2020); **80**, 410(E) (2020).
[16] A. Keshavarzi, D. Nomura, and T. Teubner, Phys. Rev. D **101**, 014029 (2020).
[17] G. Colangelo, M. Davier, A. X. El-Khadra, M. Hoferichter, C. Lehner, L. Lellouch, T. Mibe, B. L. Roberts, T. Teubner, H. Wittig *et al.*, arXiv:2203.15810.
[18] S. Borsanyi, Z. Fodor, J. N. Guenther, C. Hoelbling, S. D. Katz, L. Lellouch, T. Lippert, K. Miura, L. Parato, K. K. Szabo *et al.*, Nature (London) **593**, 51 (2021).
[19] M. Cè, A. Gérardin, G. von Hippel, R. J. Hudspith, S. Kuberski, H. B. Meyer, K. Miura, D. Mohler, K. Ottnad, P. Srijit *et al.*, arXiv:2206.06582.
[20] C. Alexandrou, S. Bacchio, P. Dimopoulos, J. Finkenrath, R. Frezzotti, G. Gagliardi, M. Garofalo, K. Hadjiyiannakou, B. Kostrzewa, K. Jansen *et al.*, arXiv:2206.15084.
[21] B. Abi *et al.* (Muon $g-2$ Collaboration), Phys. Rev. Lett. **126**, 141801 (2021).
[22] G. W. Bennett *et al.* (Muon $g-2$ Collaboration), Phys. Rev. D **73**, 072003 (2006).
[23] Y. S. Tsai, Phys. Rev. D **4**, 2821 (1971); **13**, 771(E) (1976).
[24] V. Cherepanov and S. Eidelman, Nucl. Phys. B, Proc. Suppl. **218**, 231 (2011).
[25] D. Gómez Dumm and P. Roig, Phys. Rev. D **86**, 076009 (2012).
[26] P. Roig, Ph.D. thesis, University of Valéncia, 2010 [arXiv:1301.7626].
[27] A. Sirlin, Nucl. Phys. **B71**, 29 (1974); Rev. Mod. Phys. **50**, 573 (1978); Rev. Mod. Phys. **50**, 905 (1978); Nucl. Phys. **B196**, 83 (1982); W. J. Marciano and A. Sirlin, Phys. Rev. Lett. **56**, 22 (1986); Phys. Rev. Lett. **61**, 1815 (1988); Phys. Rev. Lett. **71**, 3629 (1993); J. Erler, Rev. Mex. Fis. **50**, 200 (2004).
[28] K. Inami *et al.* (Belle Collaboration), Phys. Lett. B **672**, 209 (2009).
[29] A. Antonelli *et al.* (DM2 Collaboration), Phys. Lett. B **212**, 133 (1988).
[30] S. I. Dolinsky, V. P. Druzhinin, M. S. Dubrovin, V. B. Golubev, V. N. Ivanchenko, E. V. Pakhtusova, A. N. Peryshkin, S. I. Serednyakov, Y. M. Shatunov, V. A. Sidorov *et al.*, Phys. Rep. **202**, 99 (1991).
[31] R. R. Akhmetshin *et al.* (CMD-2 Collaboration), Phys. Lett. B **489**, 125 (2000).
[32] B. Aubert *et al.* (*BABAR* Collaboration), Phys. Rev. D **76**, 092005 (2007); **77**, 119902 (2008).
[33] V. M. Aulchenko *et al.* (SND Collaboration), Phys. Rev. D **91**, 052013 (2015).
[34] M. N. Achasov, V. M. Aulchenko, A. Y. Barnyakov, K. I. Beloborodov, A. V. Berdyugin, D. E. Berkaev, A. G. Bogdanchikov, A. A. Botov, T. V. Dimova, V. P. Druzhinin *et al.*, Int. J. Mod. Phys. Conf. Ser. **35**, 1460388 (2014).
[35] M. N. Achasov, A. Y. Barnyakov, K. I. Beloborodov, A. V. Berdyugin, D. E. Berkaev, A. G. Bogdanchikov, A. A. Botov, T. V. Dimova, V. P. Druzhinin, V. B. Golubev *et al.* Phys. Rev. D **97**, 012008 (2018).
[36] S. S. Gribanov, A. S. Popov, R. R. Akhmetshin, A. N. Amirkhanov, A. V. Anisenkov, V. M. Aulchenko, V. S. Banzarov, N. S. Bashtovoy, D. E. Berkaev, A. E. Bondar *et al.*, J. High Energy Phys. 01 (2020) 112.
[37] L. Y. Dai, J. Portolés, and O. Shekhovtsova, Phys. Rev. D **88**, 056001 (2013).
[38] W. Qin, L. Y. Dai, and J. Portolés, J. High Energy Phys. 03 (2021) 092.
[39] E. A. Garcés, M. Hernández Villanueva, G. López Castro, and P. Roig, J. High Energy Phys. 12 (2017) 027.
[40] J. A. Miranda and P. Roig, J. High Energy Phys. 11 (2018) 038.
[41] V. Cirigliano, A. Falkowski, M. González-Alonso, and A. Rodríguez-Sánchez, Phys. Rev. Lett. **122**, 221801 (2019).
[42] J. Rendón, P. Roig, and G. Toledo Sánchez, Phys. Rev. D **99**, 093005 (2019).
[43] S. Gonzàlez-Solís, A. Miranda, J. Rendón, and P. Roig, Phys. Rev. D **101**, 034010 (2020).
[44] S. Gonzàlez-Solís, A. Miranda, J. Rendón, and P. Roig, Phys. Lett. B **804**, 135371 (2020).
[45] M. A. Arroyo-Ureña, G. Hernández-Tomé, G. López-Castro, P. Roig, and I. Rosell, Phys. Rev. D **104**, L091502 (2021).
[46] M. A. Arroyo-Ureña, G. Hernández-Tomé, G. López-Castro, P. Roig, and I. Rosell, J. High Energy Phys. 02 (2022) 173.
[47] V. Cirigliano, D. Díaz-Calderón, A. Falkowski, M. González-Alonso, and A. Rodríguez-Sánchez, J. High Energy Phys. 04 (2022) 152.
[48] E. Kou *et al.* (Belle-II Collaboration), Prog. Theor. Exp. Phys. **2019**, 123C01 (2019); **2020**, 029201(E) (2020).
[49] S. Descotes-Genon and B. Moussallam, Eur. Phys. J. C **74**, 2946 (2014).
[50] R. Escribano, S. Gonzàlez-Solís, and P. Roig, Phys. Rev. D **94**, 034008 (2016).
[51] V. Cirigliano, J. Jenkins, and M. González-Alonso, Nucl. Phys. **B830**, 95 (2010).
[52] T. Bhattacharya, V. Cirigliano, S. D. Cohen, A. Filipuzzi, M. González-Alonso, M. L. Graesser, R. Gupta, and H. W. Lin, Phys. Rev. D **85**, 054512 (2012).
[53] V. Cirigliano, M. González-Alonso, and M. L. Graesser, J. High Energy Phys. 02 (2013) 046.
[54] V. Cirigliano, S. Gardner, and B. Holstein, Prog. Part. Nucl. Phys. **71**, 93 (2013).
[55] H. M. Chang, M. González-Alonso, and J. Martín Camalich, Phys. Rev. Lett. **114**, 161802 (2015).
[56] A. Courtoy, S. Baeßler, M. González-Alonso, and S. Liuti, Phys. Rev. Lett. **115**, 162001 (2015).
[57] M. González-Alonso and J. Martín Camalich, J. High Energy Phys. 12 (2016) 052.
[58] M. González-Alonso, J. Martín Camalich, and K. Mimouni, Phys. Lett. B **772**, 777 (2017).
[59] S. Alioli, V. Cirigliano, W. Dekens, J. de Vries, and E. Mereghetti, J. High Energy Phys. 05 (2017) 086.
[60] M. González-Alonso, O. Naviliat-Cuncic, and N. Severijns, Prog. Part. Nucl. Phys. **104**, 165 (2019).
[61] S. Descotes-Genon, A. Falkowski, M. Fedele, M. González-Alonso, and J. Virto, J. High Energy Phys. 05 (2019) 172.
[62] V. Cirigliano, A. Crivellin, and M. Hoferichter, Phys. Rev. Lett. **120**, 141803 (2018).

[63] F. Z. Chen, X. Q. Li, Y. D. Yang, and X. Zhang, Phys. Rev. D **100**, 113006 (2019).
[64] F. Z. Chen, X. Q. Li, and Y. D. Yang, J. High Energy Phys. 05 (2020) 151.
[65] F. Z. Chen, X. Q. Li, S. C. Peng, Y. D. Yang, and H. H. Zhang, J. High Energy Phys. 01 (2022) 108.
[66] W. Buchmuller and D. Wyler, Nucl. Phys. **B268**, 621 (1986).
[67] B. Grzadkowski, M. Iskrzynski, M. Misiak, and J. Rosiek, J. High Energy Phys. 10 (2010) 085.
[68] R. Kumar, Phys. Rev. **185**, 1865 (1969).
[69] S. Arteaga, Effective field theory analysis of the $\tau \to \eta\pi\pi\nu_\tau$ decays, Master Thesis, Cinvestav, 2019.
[70] N. N. Achasov, S. A. Devyanin, and G. N. Shestakov, Phys. Lett. **88B**, 367 (1979).
[71] S. Jadach, Z. Was, R. Decker, and J. H. Kühn, Comput. Phys. Commun. **76**, 361 (1993).
[72] S. Actis *et al.* (Working Group on Radiative Corrections and Monte Carlo Generators for Low Energies), Eur. Phys. J. C **66**, 585 (2010).
[73] G. Ecker, J. Gasser, A. Pich, and E. de Rafael, Nucl. Phys. **B321**, 311 (1989); G. Ecker, J. Gasser, H. Leutwyler, A. Pich, and E. de Rafael, Phys. Lett. B **223**, 425 (1989).
[74] C. Hanhart, B. Kubis, and J. R. Peláez, Phys. Rev. D **76**, 074028 (2007).
[75] P. A. Zyla *et al.* (Particle Data Group), Prog. Theor. Exp. Phys. **2020**, 083C01 (2020).
[76] V. Cirigliano, G. Ecker, H. Neufeld, and A. Pich, J. High Energy Phys. 06 (2003) 012.
[77] M. Jamin, J. A. Oller, and A. Pich, Nucl. Phys. **B587**, 331 (2000).
[78] M. Jamin, J. A. Oller, and A. Pich, Nucl. Phys. **B622**, 279 (2002).
[79] R. Escribano, P. Masjuan, and J. J. Sanz-Cillero, J. High Energy Phys. 05 (2011) 094.
[80] J. Schechter, A. Subbaraman, and H. Weigel, Phys. Rev. D **48**, 339 (1993); T. Feldmann and P. Kroll, Eur. Phys. J. C **5**, 327 (1998); Phys. Scr. **T99**, 13 (2002); T. Feldmann, P. Kroll, and B. Stech, Phys. Rev. D **58**, 114006 (1998); Phys. Lett. B **449**, 339 (1999); T. Feldmann, Int. J. Mod. Phys. A **15**, 159 (2000); R. Escribano and J. M. Frere, Phys. Lett. B **459**, 288 (1999); J. High Energy Phys. 06 (2005) 029.
[81] A. Guevara, P. Roig, and J. J. Sanz-Cillero, J. High Energy Phys. 06 (2018) 160.
[82] P. Roig, A. Guevara, and G. López Castro, Phys. Rev. D **89**, 073016 (2014).
[83] F. Ambrosino *et al.*, J. High Energy Phys. 07 (2009) 105.
[84] D. G. Dumm, P. Roig, A. Pich, and J. Portolés, Phys. Lett. B **685**, 158 (2010).
[85] O. Shekhovtsova, T. Przedzinski, P. Roig, and Z. Was, Phys. Rev. D **86**, 113008 (2012).
[86] I. M. Nugent, T. Przedzinski, P. Roig, O. Shekhovtsova, and Z. Was, Phys. Rev. D **88**, 093012 (2013).
[87] D. G. Dumm, P. Roig, A. Pich, and J. Portolés, Phys. Rev. D **81**, 034031 (2010).
[88] S. Weinberg, Physica (Amsterdam) **96A**, 327 (1979); J. Gasser and H. Leutwyler, Ann. Phys. (N.Y.) **158**, 142 (1984); Nucl. Phys. **B250**, 465 (1985).
[89] O. Catà and V. Mateu, J. High Energy Phys. 09 (2007) 078.
[90] I. Baum, V. Lubicz, G. Martinelli, L. Orifici, and S. Simula, Phys. Rev. D **84**, 074503 (2011).
[91] See the Supplemental Material at http://link.aps.org/supplemental/10.1103/PhysRevD.106.096016 for *Mathematica* notebook file where the terms of the unpolarized squared amplitude can be consulted or even modified.
[92] V. Shtabovenko, R. Mertig, and F. Orellana, Comput. Phys. Commun. **256**, 107478 (2020).
[93] V. Shtabovenko, R. Mertig, and F. Orellana, Comput. Phys. Commun. **207**, 432 (2016).
[94] R. Mertig, M. Bohm, and A. Denner, Comput. Phys. Commun. **64**, 345 (1991).
[95] M. K. Volkov, A. B. Arbuzov, and D. G. Kostunin, Phys. Rev. C **89**, 015202 (2014).
[96] V. Cirigliano, G. Ecker, M. Eidemüller, R. Kaiser, A. Pich, and J. Portolés, Nucl. Phys. **B753**, 139 (2006).
[97] G. 't Hooft, Nucl. Phys. **B72**, 461 (1974).
[98] G. 't Hooft, Nucl. Phys. **B75**, 461 (1974).
[99] L. Y. Dai, J. Fuentes-Martín, and J. Portolés, Phys. Rev. D **99**, 114015 (2019).
[100] P. Roig and P. Sánchez-Puertas, Phys. Rev. D **101**, 074019 (2020).
[101] J. L. Gutiérrez Santiago, G. López Castro, and P. Roig, Phys. Rev. D **103**, 014027 (2021).
[102] A. Guevara, G. L. Castro, and P. Roig, Phys. Rev. D **105**, 076007 (2022).
[103] C. Chen, C. G. Duan, and Z. H. Guo, J. High Energy Phys. 08 (2022) 144.